

# A Method for Direct Calculation of Critical Excitations in Arbitrary Two Port Systems

Katharina Feldhues, Sergey Miropolsky, Stephan Frei

TU Dortmund University

Dortmund, Germany

katharina.feldhues@tu-dortmund.de

**Abstract** — The inverse modified nodal analysis (IMNA) has been applied with success in past investigations to several EMC problems. Here a signal is defined at the system output, and the input signal necessary to produce this output signal is calculated. This way excitation signals complying with the EMC limits can be found. The method overcomes problems of typically used optimization algorithms. With a single simulation run a solution can be found. In the past the method was applied to simple passive coupling networks consisting of lumped elements. This paper deals with a significant extension. Scattering parameters matrices of two port systems have been integrated. The method, the needed date conversion algorithms and approximation procedures necessary to use S-parameter data sets in IMNA and MNA are shown. The method is applied to several test cases.

**Keywords** — scattering parameters, vector fitting approximation, two-port system, modified nodal analysis (MNA), inverse modified nodal analysis (IMNA)

## I. INTRODUCTION

Electrical circuit simulators typically use the modified nodal analysis (MNA) [1]. This method allows calculating the response on an input stimulus at all circuit nodes. In some application cases the stimulus signal is not known, but a desired output signal can be specified. In such a case the inverse modified nodal analysis (IMNA) [2] can be used to calculate the initial stimulus waveform at a specified input node that produces a given signal at an output circuit node.

Passive linear systems can be described in terms of network parameters. Methods are known to approximate a network parameter dataset as a state space model, which can be directly implemented in the matrices of both MNA and IMNA methods. This paper describes the usage of such state space models based on network parameters. The method is described in details and verified on several sample cases.

## II. THEORETICAL BACKGROUND

This section provides the basics of network scattering parameters. The approximation to state-space model and the application of the model in the MNA and IMNA equation system are discussed. A short description of the inverse modified nodal analyses is presented.

### A. Scattering Parameters of a Two-Port Circuit

Network parameters are often used to characterize linear passive systems in frequency domain. Many electrical circuit

simulators contain built-in features or tools to simulate directly the S-parameter datasets in a circuit.

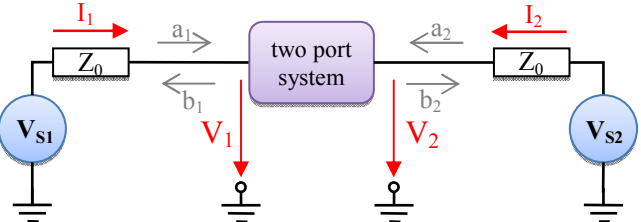


Figure 1. Two port system S-Parameter extraction circuit

A two-port system shown in fig. 1 can be analyzed with the incident ( $a_1$  and  $a_2$ ) and reflected ( $b_1$  and  $b_2$ ) power waves as follows [3]:

$$a_i = \frac{V_i + Z_0 I_i}{2\sqrt{Z_0}} ; b_i = \frac{V_i - Z_0 I_i}{2\sqrt{Z_0}} \quad (1) \quad (2)$$

The scattering parameters are defined in terms of these power waves [4]. Assuming that the  $Z_0 I_i$  term is the voltage across the  $Z_0$  impedance, we can simplify (1) (2) and build the S-parameter matrix as following:

$$\mathbf{S} = \begin{bmatrix} S_{11} & S_{21} \\ S_{12} & S_{22} \end{bmatrix} = \begin{bmatrix} \frac{2V_{11} - V_{S1}}{V_{S1}} & \frac{2V_{12}}{V_{S2}} \\ \frac{2V_{21}}{V_{S2}} & \frac{2V_{22} - V_{S2}}{V_{S2}} \end{bmatrix} \quad (3)$$

In the equation above the  $V_{ji}$  refers to port voltage  $V_j$  produced by unit amplitude  $V_{Si}$ , with  $V_{Sk(k \neq i)} = 0$ . The simulation run has to be repeated once with each port active (sending), the remaining ports are passive (receiving), and the port voltages must be calculated.

The scattering parameters of any passive circuit can be calculated in this way. The port amplitudes can be calculated to correspond to specific forward power values. The matrix can be extended to any number of ports. In the latter case the corresponding number of simulation runs (one per port) will be necessary whereby the matrix inversion is only necessary once a time in the MNA.

## B. Translation into State Space Model

The S-parameter dataset given for discrete frequencies can be directly implemented in the MNA or IMNA for AC analysis. For TD analysis the dataset can be approximated with e.g. Vectfit [5] and a state space model of the following type can be generated.

$$\dot{\mathbf{z}} = \mathbf{A}_S \cdot \mathbf{z} + \mathbf{B}_S \cdot \mathbf{a} \quad (4)$$

$$\mathbf{b} = \mathbf{C}_S \cdot \mathbf{z} + \mathbf{D}_S \cdot \mathbf{a} \quad (5)$$

The incident power wave vector  $\mathbf{a}$  is the input and the reflected power wave vector  $\mathbf{b}$  is the output of the state space model. The vector  $\mathbf{z}$  contains the internal state space variables.

Another option to use the system description in the MNA or IMNA is to translate the S-parameters into Y-parameters. Also the Y-parameters can be approximated with Vectfit and a state space model can be generated.

$$\dot{\mathbf{z}} = \mathbf{A}_Y \cdot \mathbf{z} + \mathbf{B}_Y \cdot \mathbf{v} \quad (6)$$

$$\mathbf{i} = \mathbf{C}_Y \cdot \mathbf{z} + \mathbf{D}_Y \cdot \mathbf{v} \quad (7)$$

The variables  $\mathbf{i}$ ,  $\mathbf{v}$  and  $\mathbf{z}$  denote the vectors of port currents, port voltages and internal state space variables. In both systems the system matrix  $\mathbf{A}$ , input matrix  $\mathbf{B}$ , output matrix  $\mathbf{C}$  and feed through matrix  $\mathbf{D}$  describe the behavior of the original two port system. It is also possible to build a state space model in terms of Z-parameters (not shown here).

## C. State Space Model in Modified Nodal Analysis

The MNA allows calculating the time-dependent node voltages and selected currents for a given electric circuit. This is a common approach used in electrical circuit simulators [6], [7]. The following equation is used for the time domain analysis:

$$\mathbf{C} \cdot \dot{\mathbf{x}}(t) + \mathbf{G} \cdot \mathbf{x}(t) = \mathbf{w}(t) \quad (8)$$

Here the vector  $\mathbf{x}$  contains  $M$  unknown quantities and the vector  $\mathbf{w}$  includes  $M$  known values. With the matrices  $\mathbf{C}$  and  $\mathbf{G}$  the electric circuit is described.

To include the state space model in the MNA the equations (1) (2), (4) and (5) have to be integrated into (8). The  $\mathbf{x}$  and  $\mathbf{w}$  vectors must be correspondingly extended. For a two port system the vectors have the following form:

$$\tilde{\mathbf{x}}^T = [\mathbf{x} \ i_{in} \ i_{out} \ a_1 \ a_2 \ b_1 \ b_2 \ \mathbf{z}_1 \ \dots \ \mathbf{z}_N] \quad (9)$$

$$\tilde{\mathbf{w}}^T = [\mathbf{w} \ 0 \ \dots \ 0] \quad (10)$$

$$\tilde{\mathbf{G}} = \begin{bmatrix} \mathbf{G} & 1 & 1 \\ 1/(2\sqrt{Z_0}) & 1/(2\sqrt{Z_0}) & -1 \\ 1/(2\sqrt{Z_0}) & -1/(2\sqrt{Z_0}) & -1 \\ 1/(2\sqrt{Z_0}) & 1/(2\sqrt{Z_0}) & -1 \\ D_{11} & D_{12} & -1 \\ D_{21} & D_{22} & -1 \\ B_{11} & B_{12} & A_{11} \\ \vdots & \vdots & \vdots \\ B_{N1} & B_{N2} & A_{NN} \end{bmatrix}$$

The  $\mathbf{C}$  and  $\mathbf{G}$  matrices have to be extended too. With the assumption that the input and output ports are connected to the corresponding circuit nodes all matrices from the state space model can be included as it is shown in fig. 2. The blue boxes represent the state space model. The red box is the original MNA matrix. The green box considers the Kirchhoff's nodal law (sum of currents flowing into and out of the node must be zero). The purple box defines the correlation between power waves, voltage and current values. The new matrices have the size of  $M+N+6$ , where  $N$  is the number of state space variables. Two more lines are necessary to represent the currents in a two-port system and four more lines define the power waves. The matrix used for MNA simulation is explained more in detail in [1], [6] and [7].

As it was already mentioned, the Y-parameters could also be used. The equations (6) and (7) have to be included into (8).

$$\tilde{\mathbf{x}}^T = [\mathbf{x} \ i_{in} \ i_{out} \ \mathbf{z}_1 \ \mathbf{z}_2 \ \dots \ \mathbf{z}_N] \quad (11)$$

$$\tilde{\mathbf{w}}^T = [\mathbf{w} \ 0 \ \dots \ 0] \quad (12)$$

The extended  $\mathbf{C}$  and  $\mathbf{G}$  matrices have  $M+N+2$  elements. The matrix elements defining the incident and scattered waves are not necessary in this case, however to reach the same accuracy in terms of Y-parameters a higher model order is mostly necessary.

Furthermore a wave simulation can be performed with the S-parameters directly. This is possible under the assumption that the external circuit contains  $50\Omega$  sources and terminations only. In this case only the waves and internal state variables have to be considered:

$$\tilde{\mathbf{x}}^T = [a_1 \ a_2 \ b_1 \ b_2 \ \mathbf{z}_1 \ \dots \ \mathbf{z}_N] \quad (13)$$

$$\tilde{\mathbf{w}}^T = [\mathbf{w} \ 0 \ \dots \ 0] \quad (14)$$

The matrices  $\mathbf{C}$  and  $\mathbf{G}$  can be reduced to its state space component (blue box in fig. 2) with four additional lines for the incident and scattered waves. Here the input and output signals have to be defined in terms of incident and scattered waves.

Moreover, the incident waves will always be zero at the ports terminated with matched impedances, thus the corresponding lines in the matrices can be neglected. If the output signals at some outputs are not of interest, the signal transfer to these ports can be neglected without loss of simulation accuracy, and the corresponding lines in the system matrix can be removed. Therefore, in such simulation case the matrices can be reduced to the  $S_{21}$  signal transfer only.

Figure 2. Structure of the  $\mathbf{C}$  and  $\mathbf{G}$  matrix

$$\tilde{\mathbf{C}} = \begin{bmatrix} \mathbf{c} \\ \vdots \\ -1 & \ddots & -1 \end{bmatrix}$$

#### D. Inverse Modal Analyses

The inverse modal analysis (IMNA) is based on the MNA. With this method it is possible to calculate an unknown voltage source  $V_x$  (e.g. a disturbing pulse) in a system when a nodal voltage  $V_{\text{predefined}}$  (e.g. a victim immunity threshold voltage) is given. The predefined signal could appear at any node of the investigated electrical circuit. In the IMNA the unknown voltage is one of the variables in the vector  $\mathbf{x}$ . The unknown source voltage ( $V_x$ ) corresponds to an unknown current ( $I_x$ ). With these unknown signals the vector  $\mathbf{x}$  is defined as follows [2], [8]:

$$\tilde{\mathbf{x}}^T = [\mathbf{x}^T \quad I_x \quad V_x] \quad (15)$$

This leads to a modification of the matrices  $\mathbf{C}$  and  $\mathbf{G}$ . The matrix  $\mathbf{C}$  has to be extended with two rows and columns with zeros because the disturbance source does not influence the derivative. With the assumption that the nodal voltage signal  $V_{\text{predefined}}$  is given at the  $k$ -th node

$$e_k = V_{\text{predefined}} \quad (16)$$

and the corresponding unknown voltage source  $V_x$  is connected between node  $l$  and  $m$ ,

$$e_l - e_m = V_x \quad (17)$$

the matrix  $\mathbf{G}$  is modified in the following way. The stamps for the voltage source (orange), the unknown source (red), and the given voltage ( $V_{\text{predefined}}$ ) (blue) are considered in the matrix  $\mathbf{G}$  and the vector  $\mathbf{w}$  [2], [8].

$$\tilde{\mathbf{G}} = \begin{matrix} l & m & k & M+1 & M+2 \\ \begin{matrix} l \\ m \\ k \\ M+1 \\ M+2 \end{matrix} & \mathbf{G} & \begin{matrix} 1 \\ -1 \\ \text{orange} \end{matrix} & \begin{matrix} -1 \\ -1 \end{matrix} & \begin{matrix} -1 \\ \text{red} \end{matrix} \end{matrix} \quad (18)$$

$$\tilde{\mathbf{w}}^T = [\mathbf{w}^T \quad 0 \quad V_{\text{predefined}}] \quad (19)$$

Using the MNA equation system (8) as a basis, the differential equation system for the IMNA can be written.

$$\tilde{\mathbf{C}} \cdot \dot{\tilde{\mathbf{x}}}(t) + \tilde{\mathbf{G}} \cdot \tilde{\mathbf{x}}(t) = \tilde{\mathbf{w}}(t) \quad (20)$$

This system can be solved with well-known algorithms [7].

### III. VERIFICATION AND APPLICATION

In this section the results, including calculation of the scattering and admittance parameters, numerical approximation, MNA and IMNA analyses are shown. In all cases two port systems are discussed. The S-parameters are generated with simulation methods using MNA. The S- or Y-parameters are approximated with vector fitting to a state space model. The following circuit is used for all cases.

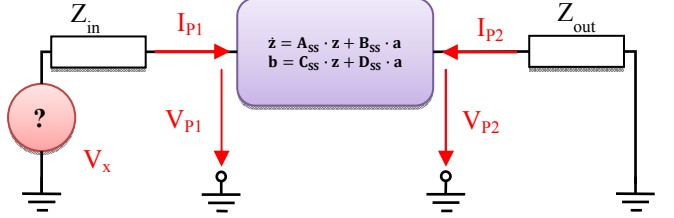


Figure 3. Simulation circuit of a two-port system

The model can be used in both MNA and IMNA. For the IMNA the output voltage  $V_{P2}$  is defined and the voltage source  $V_x$  is unknown. The goal of the IMNA analysis is to calculate a voltage source signal when a signal at the node P2 is given.

#### A. First Case: Passive RLC Circuit

A simple circuit shown in fig. 4 will be considered in the first case. The S-parameters of the circuit are generated as discussed in section II.A, transformed into Y-parameters and approximated with Vectfit [5].

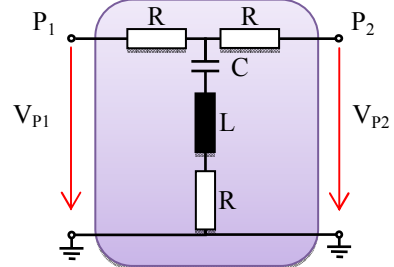


Figure 4. First study case: passive RLC circuit

The approximated and original Y-parameters are shown in the fig. 5. A very good accuracy of the approximation can be observed.

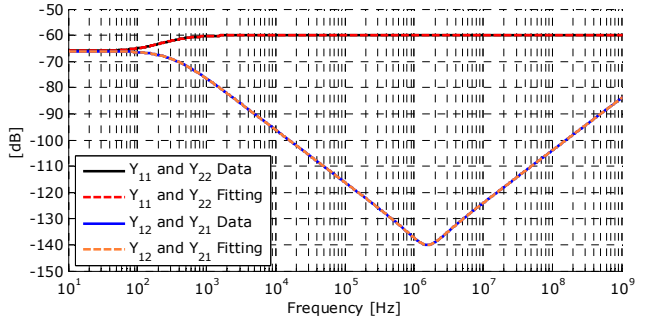


Figure 5. Admittance (Y) parameters: original dataset vs. approximation

The circuit shown in fig. 3 with the state space model of the circuit in fig. 4 is used for the analysis. At the first step the system is simulated with the normal MNA. A sample pulse of 10 V amplitude with 1 ns rising edge (fig. 6) is applied to the input port. The voltage responses at all nodes are simulated. The simulated response at the second port ( $V_{P2}$ ) is then used as an input value for IMNA. The signal at the system input port is calculated and compared to the initially-applied pulse.

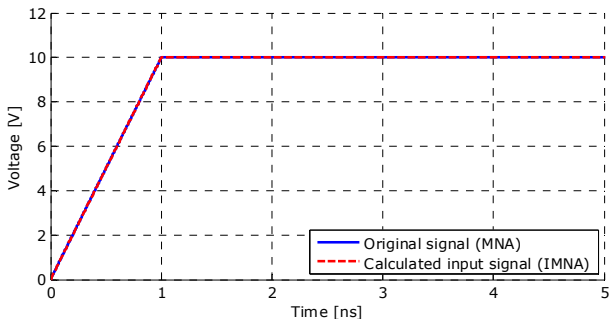


Figure 6. Source voltage pulse in the first case

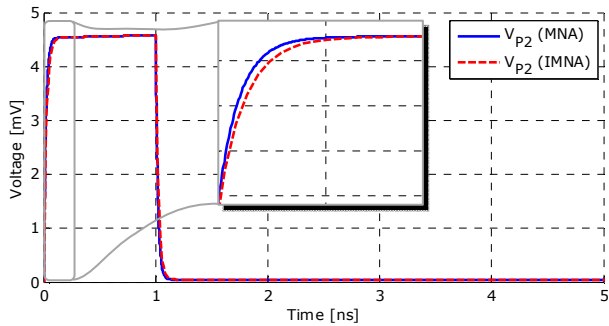


Figure 7. Voltage at the output port of two-port system (zoomed)

The signals restored with the IMNA from known response signal show good correlation with the initial MNA simulation. The rising edge shows smaller deviations from the original signal. This deviation is presumably caused by insufficiently accurate numerical approximation.

#### B. Second Case: Measurement with a Current Sensor

The second system analyzed is a more complex setup. A cable is placed over a reference ground plane. The source is attached to one cable port. The second cable port is terminated with a RC network. A current sensor is used to measure the current at the termination (fig. 8).

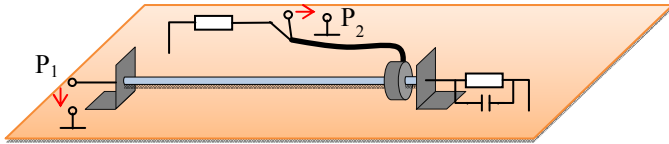


Figure 8. Second study case: current sensor measurement on cable harness

The system is again considered as a two-port, with first port located at the source, and the second port at the current sensor output. The signal transfer in terms of S-parameters is simulated, converted into a Y-parameter representation, and approximated with Vectfit [5]. The MNA and IMNA matrices are assembled in the same way as before.

The original pulse, same as in the previous study case (fig. 6), is applied to the input port. The response signals are computed at other circuit nodes, including the termination and the current sensor output. The same procedure is used to restore the original signal at the input port. The equivalent circuit diagram for the simulation is shown in fig. 9.

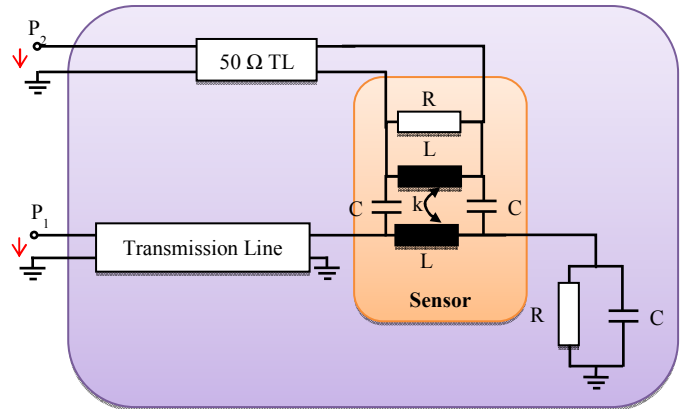


Figure 9. Equivalent circuit model for second study case

The simulated curves for the input port are shown in fig. 10. As in the previous case, a very good accuracy of the inverse simulation method can be observed. Smaller oscillations can be observed at the restored signal.

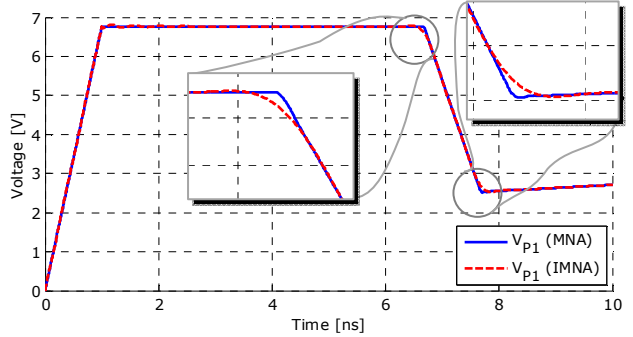


Figure 10. Voltage at the input port: initial pulse vs IMNA-restored pulse

#### C. Third Case: Antenna Measurement of Cable Harness

In this section a sample practical application, an antenna measurement setup is analyzed. A cable harness is located on a table and an antenna is used to measure the radiated field.

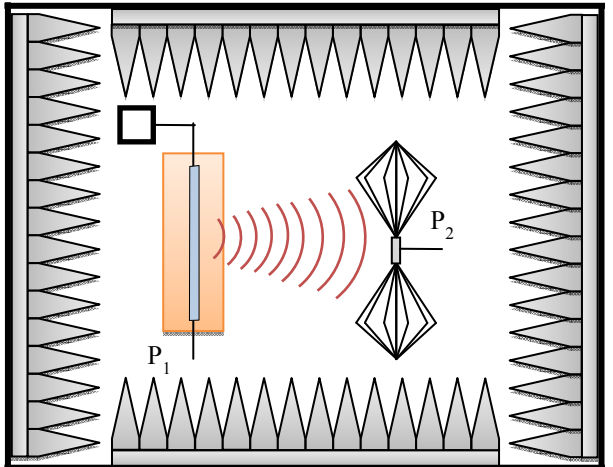


Figure 11. Third case: antenna measurement of cable harness

The system is analyzed by simulation only. The S-parameters are generated by field computation. First the

system (fig. 12) is analyzed in the same way as the systems in III.A and III.B. The MNA and IMNA simulations are performed. The second experiment is based on the same simulated S-parameter dataset. In this case the IMNA is used directly with a frequency domain voltage defined over the antenna port and the corresponding signal at port 1 is calculated.

### 1) Case 1: Pulse response of the antenna setup

The S-parameter dataset of the antenna measurement setup calculated with the MoM method and the S-parameters approximated with Vectfit are shown in fig. 12.

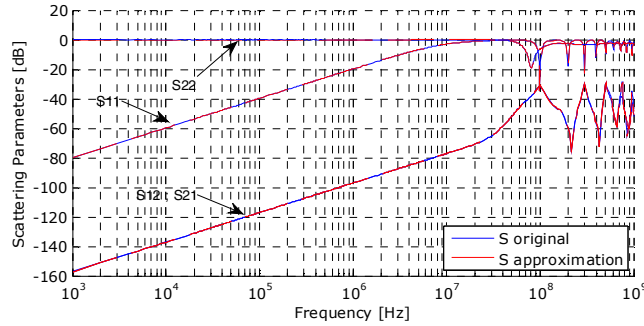


Figure 12. Scattering parameters of the antenna setup

The first experiment is the same as in section III. First the system is analyzed with the MNA and the responses at the second port are computed. Afterwards the IMNA analysis is performed and both results are compared. Again, a very high accuracy of the inverse simulation can be observed.

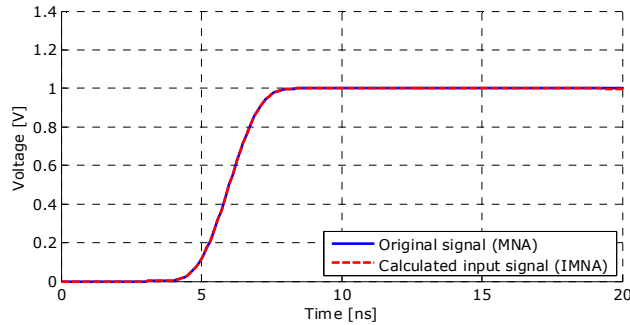


Figure 13. Source voltage pulse in antenna setup simulation (IV.A)

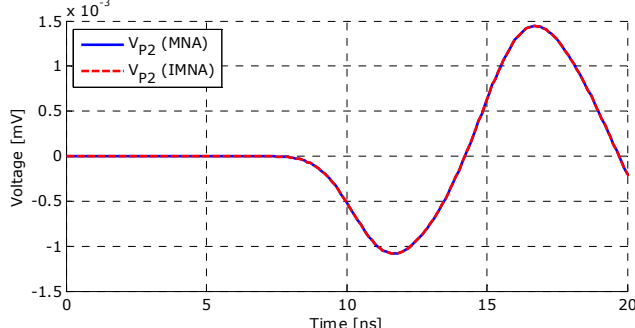


Figure 14. Voltage at the antenna measurement port (IV.A)

### 2) Case 2: Radiation thresholds prediction

A frequency domain signal can be defined directly at the antenna port using threshold level specified by radiation standards (e.g. CISPR 25 [9]). The peak limits for radiated disturbances in the specific frequency ranges are:

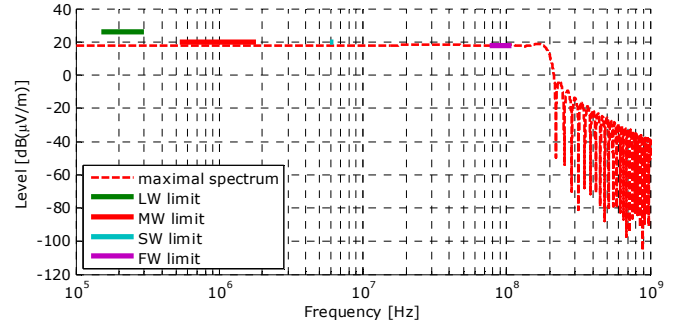


Figure 15. Peak limits for radiation according to CISPR 25 Class 5

This maximal spectrum is transformed into the time domain. The corresponding time domain signal is cropped and the time axis is shifted so that the signal is zero at the edges of the discussed time window as shown in fig. 16.

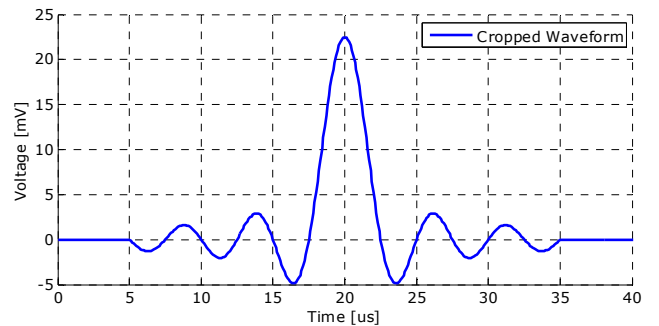


Figure 16. Cropped time domain signal for IMNA simulation

The source voltage at port 1, necessary to generate the signal (fig. 16) at port 2, is calculated with IMNA (fig. 17).

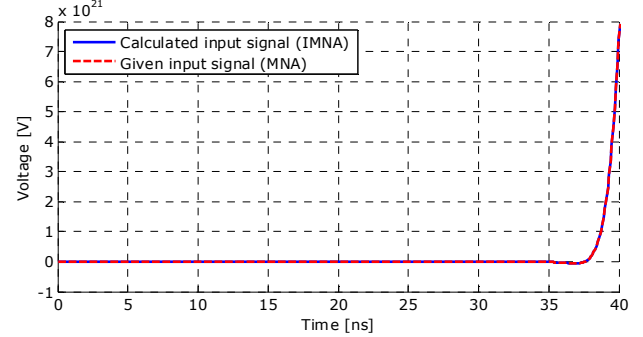


Figure 17. Source voltage signal calculated with IMNA

The resulting source voltage shows the orders of  $10^{21}$ , which is unphysical. Nevertheless, the voltage is applied in simulation to the system input in MNA to verify, if the same output signal is obtained.

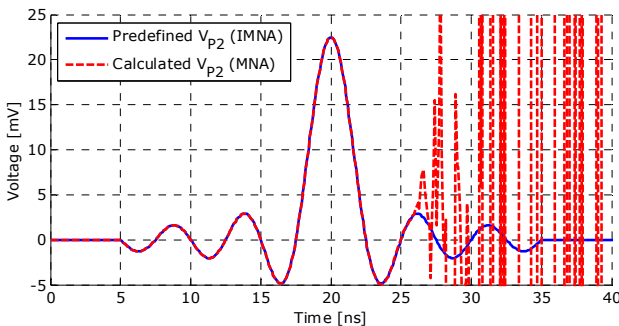


Figure 18. Output port signal produced by the calculated source signal

The output waveform obtained with the calculated input voltage (fig. 18) fits the expected values up to 25 ns. Afterwards stability problems can be observed.

The further analysis has shown that the instability problem might be caused by a weak coupling from input to output port (down to -160 dB, see fig. 12). This is typical for the analyzed antenna setup in LF range. The strong attenuation of the discussed system in MNA ( $b_2/a_1$ ) results in the amplification of the same magnitude for IMNA analysis ( $a_1/b_2$ ).

To solve the weak coupling issue, the model was extended with an additional high-ohmic DC coupling path (additional resistor). The resistor value was selected in order not to affect the  $S_{21}$  signal transfer in the needed frequency range. The IMNA simulation was performed again with additional high-ohmic DC coupling path (fig. 19).

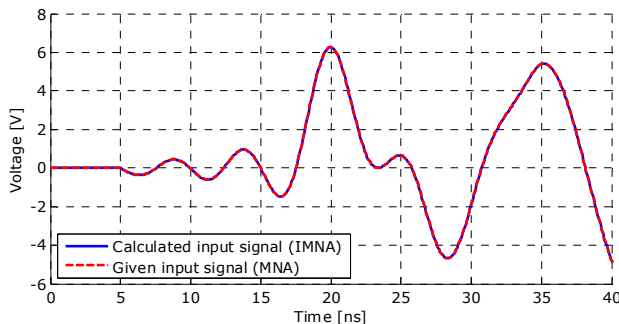


Figure 19. Source voltage signal calculated with enforced LF coupling

The source voltage pulse calculated for the system with stronger DC coupling agrees well with the signal from MNA analysis.

#### IV. SUMMARY AND OUTLOOK

In the paper a method to find critical excitation pulse shapes based on an inverse MNA (IMNA) is extended for including S-parameter datasets from measurement or field calculation. The dataset is approximated to a state space model and included in the IMNA equation system. Input signals necessary to produce a predefined output signal can be found directly. This way e.g. the thresholds given in EMC standards can be reached exactly by synthesizing the input signals. The integration of measurement data from a network analyzer or

3D field computation makes the method applicable to complex coupling problems. The method can be extended to systems with an arbitrary port number.

The method is verified in this paper on several cases, where the datasets were generated with simulation. A very good accuracy of the method could be observed in cases, where the output signals are initially generated by a known input signal. Several issues have been observed in the IMNA simulation for arbitrary output signals. The issues could be partially solved by enforcing the weak coupling of the system, especially in the LF range. The question of inverse simulation causality for the systems with time delays has to be investigated more in detail. Moreover, in further work the application of IMNA for more complex setups has to be considered.

#### ACKNOWLEDGMENT

The work in this paper was partly funded by the European Union (EFRE), the North Rhine-Westphalian Ministry for Economic Affairs, Energy, Building, Housing and Transport and the North Rhine-Westphalian Ministry for Climate Protection, Environment, Agriculture, Conservation and Consumer Affairs as part of the TIE-IN project.

#### REFERENCES

- [1] J. Vlach und K. Singhal, Computer Methods for Circuit Analysis and Design, Springer, 1994.
- [2] K. Feldhues, „Entwicklung einer Methode zur inversen Bestimmung von Störgrenzwerten basierend auf Simulationsmodellen der kritischen Koppelstrecken und Datenübertragungssystemen,“ *Elektromagnetische Verträglichkeit*, pp. 119-126, 2012.
- [3] O. Zinke und H. Brunswig, Hochfrequenztechnik 1, 6. Auflage Hrsg., Springer Verlag, 2000.
- [4] R. Mavaddat, Network scattering parameters, Singapore: World Scientific, 1996.
- [5] B. Gustavsen, „Rational Approximation of frequency domain responses by vector fitting,“ *IEEE Transaction on power delivery*, Bd. Vol. 14, Nr. No. 3, July 1999.
- [6] W. J. McCalla, Fundamentals of computer-aided circuit simulation, Springer, 1987.
- [7] J. Ogradzki, Circuit Simulation Methods and Algorithms, C. Press, Hrsg., 1944.
- [8] K. Feldhues, K. Siebert und S. Frei, „Determination of Critical Coupling Parameters Using Inverse Methods,“ Rom, 2012.
- [9] „CISPR 25 Ed.3“. 2007.
- [10] A. E. R. P. A. B. Chung-Wen Ho, „The modified nodal approach to network analysis,“ *IEEE Transactions on circuits and systems*, pp. 504-509, Juni 1976.
- [11] F. Gustraus, Hochfrequenztechnik, München: Carl Hanser Verlag, 2011.